Journal of Applied Polymer Science

Effects of compatibilizer on the morphological, mechanical, and rheological properties of poly(methyl methacrylate)/poly(*N*-methyl methacrylimide) blends

Ji Mun Kim,[1] Myung Geun Jang,[1] Dong Hyup Park,[2] Woo Nyon Kim[1]

[1]Department of Chemical and Biological Engineering, Korea University, Anam-dong Seoul 136-713, South Korea

[2]Polymer Materials Team, Convergence Technology Division, Korea Conformity Laboratory, 199 Gasan Digital 1-ro, Geumcheon-gu Seoul 153-803, South Korea

Correspondence to: W. N. Kim (E-mail: kimwn@korea.ac.kr)

ABSTRACT: The effects of compatibilizer on the morphological, thermal, mechanical, and rheological properties of poly(methyl methacrylate) (PMMA)/poly(*N*-methyl methacrylimide) (PMMI) (70/30) blends were investigated. The compatibilizer used in this study was styrene–acrylonitrile–glycidyl methacrylate (SAN-GMA) copolymer. Morphological characterization of the PMMA/PMMI (70/30) blend with SAN-GMA showed a decrease in PMMI droplet size with an increase in SAN-GMA. The glass-transition temperature of the PMMA-rich phase became higher when SAN-GMA was added up to 5 parts per hundred resin by weight (phr). The flexural and tensile strengths of the PMMA/PMMI (70/30) blend increased with the addition of SAN-GMA up to 5 phr. The complex viscosity of the PMMA/PMMI (70/30) blends increased when SAN-GMA was added up to 5 phr, which implies an increase in compatibility between the PMMA and PMMI components. From the weighted relaxation spectrum, which was obtained from the storage modulus and loss modulus, the interfacial tension of the PMMA/PMMI (70/30) blend was calculated using the Palierne emulsion model and the Choi-Schowalter model. The results of the morphological, thermal, mechanical, and rheological studies and the values of the interfacial tension of the PMMA/PMMI (70/30) blends suggest that the optimum compatibilizer concentration of SAN-GMA is 5 phr. © 2016 Wiley Periodicals, Inc. J. Appl. Polym. Sci. **2016**, *133*, 43856.

KEYWORDS: blends; compatibilization; morphology; rheology; thermal properties

Received 6 November 2015; accepted 25 April 2016

DOI: 10.1002/app.43856

INTRODUCTION

Polymer blending provides an efficient way to improve the properties of polymers. Therefore, many studies concerning polymer blending and composites have been carried out over the last few decades. Several studies have been done on polymer blends and composites of poly(methyl methacrylate) (PMMA) with other polymers or fillers, such as poly(vinylidene fluoride),[1–4] polyamide-6,[5,6] polystyrene (PS),[7,8] poly(styrene-*co*-acrylonitrile) (SAN),[9,10] polycarbonate,[11,12] poly(vinyl chloride),[13,14] poly(ethylene terephthalate),[15,16] poly(lactic acid),[17–20] polyethylene,[21,22] polypropylene,[23,24] poly(propylene carbonate),[25,26] poly(ethylene oxide),[27,28] and various types of fillers such as carbon nanotubes[4,6,29,30] and graphene.[31]

PMMA is an amorphous transparent thermoplastic that has many industrial applications. PMMA has lower thermal stability and fewer desirable mechanical properties than poly(*N*-methyl methacrylimide) (PMMI). PMMI has a high heat deflection temperature and high mechanical strength.[32] Therefore, we hypothesized that blending PMMA with PMMI would overcome the drawbacks of PMMA. Blends of PMMA with various polymers have been studied by many investigators; however, PMMA/PMMI blends have not previously been studied in depth.

The use of a copolymer as a compatibilizer is a good method for improving the compatibility of polymer blends, since blocks of grafted copolymer have intermolecular interactions with each component of polymer blends.[7,26,33] In studies on PMMA and PS blends with styrene–ethylene–butylene–styrene-*g*-maleic anhydride (SEBS-*g*-MAH) copolymer as a compatibilizer, Mallick and Khatua observed a reduction in the domain size of the dispersed PS phase in the PMMA matrix compared to that in the blend without compatibilizer.[7] In studies on PMMA and poly(2,6-dimethyl-*p*-phenylene oxide) (PPO) blends by Eklind *et al.*,[33] poly(styrene-*g*-ethylene oxide) copolymer was used as a compatibilizer. They observed that the copolymer reduced the dispersed phase size of the PMMA/PPO blend.

In this study, styrene–acrylonitrile–glycidyl methacrylate (SAN-GMA) copolymer was used as a compatibilizer. Since the GMA in SAN-GMA contains a carbonyl group, making it highly polar, we expected it to have a polar–polar interaction with the carbonyl group in PMMI.[34] It will also interact with PMMA: the intramolecular force between the acrylonitrile and styrene groups of SAN enables a PMMA/SAN blend to be miscible.[9,35,36] Thus, it was expected that SAN-GMA copolymer would be a good compatibilizer and improve the thermal and mechanical properties of PMMA/PMMI blends. The effects of compatibilizer content on the morphological, thermal, mechanical, and rheological properties of a PMMA/PMMI (70/30) blend were investigated. The interfacial tension between PMMA and PMMI was determined from the weighted relaxation spectra using the Palierne emulsion model, and the interfacial tension values were found to be correlated with the degree of compatibility.

EXPERIMENTAL

Materials

The materials used in this study were obtained from commercial sources. PMMA (grade HP 202-G1) was supplied by LG MMA Co. (Seoul, South Korea). PMMI (grade ACRYMID TT-50) was supplied by Evonik Industries (Parsippany, NJ). The densities of PMMA and PMMI were 1.18 and 1.21 g/cm^3, respectively. The glass-transition temperatures (T_g) of PMMA and PMMI were 113.4 and 155.0 °C, respectively. The number and weight average molecular weights of PMMA were 32,800 and 82,000 g/mol, respectively. For PMMI, the number and weight average molecular weights were 42,500 and 189,000 g/mol, respectively. The flexural strength of PMMA and PMMI was 93.5 and 129.5 MPa, respectively. The flexural modulus of PMMA and PMMI was 2145.0 and 3057.7 MPa, respectively. The SAN-GMA (grade SAG-002) compatibilizer was supplied by Nantong Sunny Polymer New Material Technology Co. Ltd. (China, Nantong, China). The melt index of SAN-GMA was 8.0 g/10 min, and the epoxy group content was 2.0 wt % (ASTM D1652). For comparison, poly(styrene-*co*-acrylonitrile) (SAN) was also used as a compatibilizer. The SAN (grade SAN-95 HCP) was supplied by LG Chemical Co. (Seoul, South Korea).

Sample Preparation

Blends of PMMA and PMMI were prepared by melt-mixing with SAN-GMA as a compatibilizer. The weight ratio of PMMA to PMMI was fixed at 70/30 (wt %). The concentrations of SAN-GMA tested were 0, 1, 3, 5, and 7 phr (parts per hundred resin by weight). Before melt-blending of the samples, PMMA, PMMI, and SAN-GMA were dried in a vacuum oven at 120 °C for 24 h. PMMA/PMMI/SAN-GMA blends were prepared using a twin screw extruder (Bautek Model BA-11, Seoul, South Korea) with a rotational speed of 180 rpm. The extrusion temperature was set at 130 °C in the feeding zone and 280 °C in the barrel zone. For comparison, a PMMA/PMMI (70/30) blend with the SAN copolymer as a compatibilizer was also prepared using the same method. For the morphological, rheological, thermal and mechanical measurements, blend samples were prepared using a minimax molder (Forks Township, Pennsylvania, USA) at 280 °C.

Morphology

The morphologies of the cross-sectional surfaces of the PMMA/PMMI/SAN-GMA blends were investigated with field emission scanning electron microscopy (FESEM) (Hitachi, model S-4300S, Tokyo, Japan) with a 15.0 kV accelerating voltage after platinum deposition. The surfaces of the blends were prepared by cryogenic fracturing.

Differential Scanning Calorimetry

The thermal properties of the samples were analyzed using a TA Instruments differential scanning calorimeter (DSC) (model Q200, New Castle, Delaware, USA). Temperature calibration was performed using indium ($T_m = 156.6$ °C, $\Delta H_f = 28.5$ J/g). In order to measure the T_g of the PMMA/PMMI/SAN-GMA blends, ~10 mg samples were heated in a nitrogen-rich atmosphere from 40 °C to 280 °C at a heating rate of 20 K/min. The T_g values reported here are the data obtained from the second heating scan of the samples.

NMR Spectroscopy

A ^{13}C magic angle spinning nuclear magnetic resonance (MAS NMR) spectrometer (Unity Inova 200, Varian, Palo Alto, California, USA) at a magnetic field of 4.7 T was used to characterize the PMMA/PMMI (70/30) blend with and without SAN-GMA compatibilizer. The ^{13}NMR spectra were taken by the cross-polarization (CP) method employing hexamethylbenzene as the reference.

Mechanical Properties

The flexural strength and flexural modulus of the PMMA/PMMI/SAN-GMA blends were measured at room temperature using a universal testing machine (Instron 4467, Norwood, Massachusetts, USA) according to ASTM D790. The span length and the speed of the crosshead movement were 50 mm and 1.39 mm/min, respectively. The tensile strength and tensile modulus of the blends were investigated under ambient conditions using a universal testing machine (Instron 4467). The tensile strength test was performed according to ASTM D638. The impact strength of the blends was measured by a notched Izod impact strength tester (Toyoseiki DG-IB2, Tokyo, Japan). The impact test was performed according to ASTM D256. For all of the above mechanical tests, five specimens were measured and the results were averaged.

Rheology

Dynamic frequency sweep tests were carried out using an advanced rheometric expansion system (ARES) in oscillatory shear at 10% strain in the parallel-plate arrangement with a 25 mm plate in a dry nitrogen environment. The samples were fabricated into a 1 mm thick disk. Frequency sweeps from 0.03 to 100 rad/s were performed at 250 °C, and the measurements were carried out within a linear viscoelastic range.

RESULTS AND DISCUSSION

Morphology

Figure 1(a–e) shows the scanning electron micrographs of the cryogenically fractured surfaces of PMMA/PMMI (70/30) blends with SAN-GMA concentrations of 0, 1, 3, 5, and 7 phr, respectively. Figure 2 shows the droplet size of PMMI of the PMMA/PMMI (70/30) blends with the SAN-GMA concentrations from

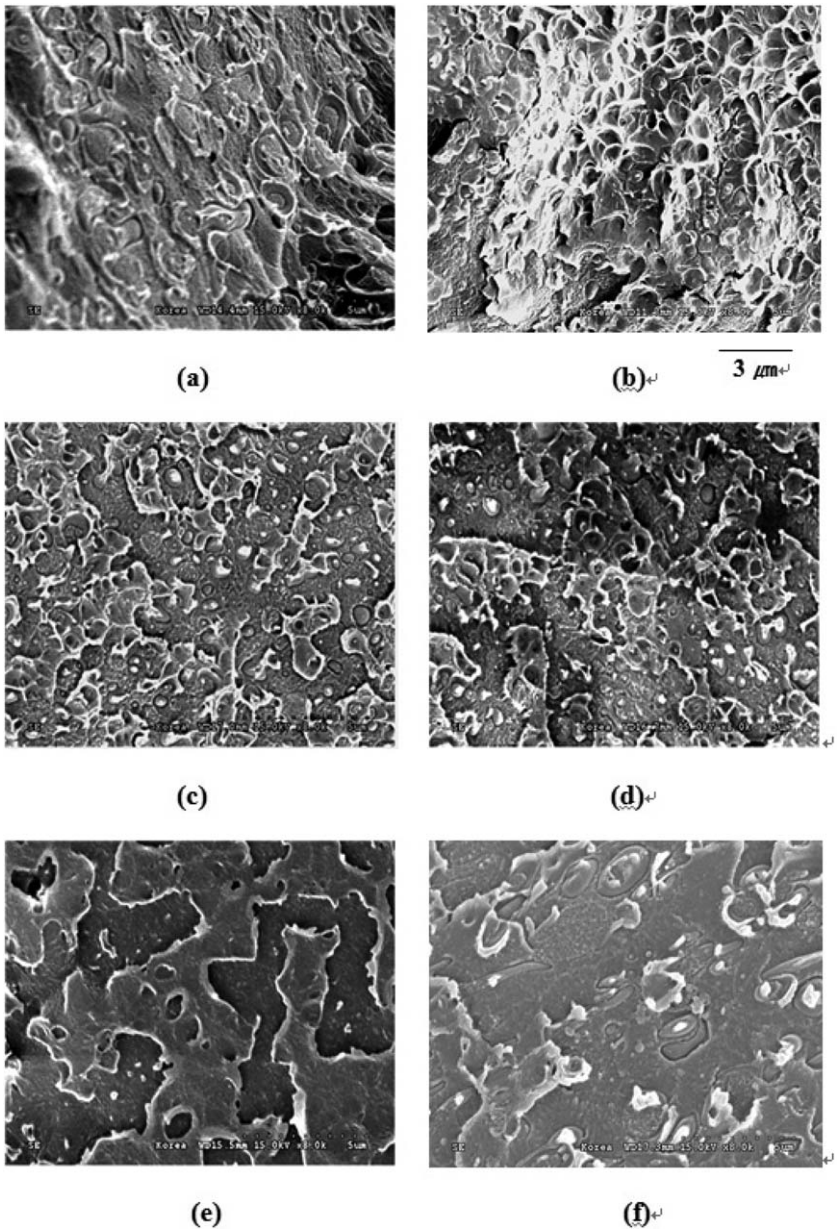

Figure 1. Scanning electron micrographs of PMMA/PMMI (70/30) blends compatibilized with SAN-GMA: (a) 0 phr, (b) 1 phr, (c) 3 phr, (d) 5 phr, (e) 7 phr. PMMA/PMMI (70/30) blends compatibilized with SAN: (f) 5 phr.

0 to 7 phr. Although it is hard to define the size of the dispersed phase because of its irregular shape and small size, it is clear that the PMMI droplet size decreases until a SAN-GMA concentration of 5 phr. This result suggests that the SAN-GMA effectively acts as a compatibilizer in the PMMA/PMMI (70/30) blends. For the blend with 7 phr SAN-GMA, however, PMMI droplet size was not significantly different from that of the blend with 5 phr SAN-GMA.

Figure 1(f) shows the scanning electron micrograph of the cryogenically fractured surfaces of PMMA/PMMI (70/30) blends with the SAN concentration of 5 phr. From Figure 1(f), the PMMI droplet size in the PMMA/PMMI blend was 0.75 μm, which was larger than that of the PMMA/PMMI blend compatibilized with the SAN-GMA. The results presented in Figure 1 suggest that the compatibility of PMMA and PMMI increases with the addition of SAN-GMA, because the size of the dispersed phase (PMMI) decreased and the phase separation between PMMA and PMMI was not pronounced when SAN-GMA was added.

Thermal Properties

Figure 3(a–e) shows the DSC thermograms of the PMMA/PMMI blends with SAN-GMA concentrations of 0, 1, 3, 5, and 7 phr, respectively. Figure 3 shows that PMMA and PMMI are partially miscible. Two glass-transition regions are observed, which we designate as T_g (PMMI), associated with PMMI-rich regions, and T_g (PMMA), associated with PMMA-rich regions. The lower T_g, T_g (PMMA), and the upper T_g, T_g (PMMI), of

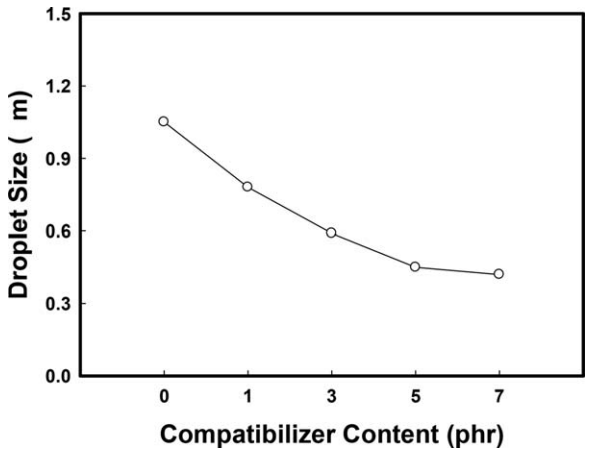

Figure 2. Droplet size of PMMA/PMMI (70/30) blends with SAN-GMA content.

the PMMA/PMMI (70/30) blends with SAN-GMA concentration are shown in Table I.

The increase in T_g (PMMA) is more pronounced than the decrease in T_g (PMMI) toward the center of the T_g of the PMMA/PMMI blends, which suggests that PMMI dissolves more readily in the PMMA-rich phase than does PMMA in the PMMI-rich phase. After the addition of SAN-GMA to the PMMA/PMMI blends, the T_g of the PMMA-rich phase shifts toward a higher temperature, most likely because of improved compatibility between PMMA and PMMI.

NMR Spectroscopy of the Blends

Figure 4(a,b) shows the ^{13}C-NMR spectra of the PMMA/PMMI (70/30) blends with and without SAN-GMA (5 phr), respectively. The NMR spectra show a carbonyl group (C═O) peak at 170.8 ppm (peak A), which indicates the existence of the ester structures of the PMMA and PMMI.[37] The peak C at 94.7 ppm represents CH_3—O, and the peak D at 51.3 ppm represents CH_2 of the PMMA and PMMI. The peak E at 44.5 ppm represents a tetravalent carbon. The peaks F and G at 29.0 and 20.1 represent a CH_3—C of the PMMA and PMMI. The peak B (125.9 ppm), which appeared only in Figure 4(a), represents a carbon peak in the aromatic group of SAN-GMA. The difference between Figures 4(a) and 4(b) is the existence of peak B, which represents carbon in the aromatic group of SAN-GMA. Since the GMA in SAN-GMA contains a carbonyl group, making it highly polar, we expect it to have a polar–polar interaction with the carbonyl group in PMMI, which may increase the compatibility between the PMMA and PMMI phases.

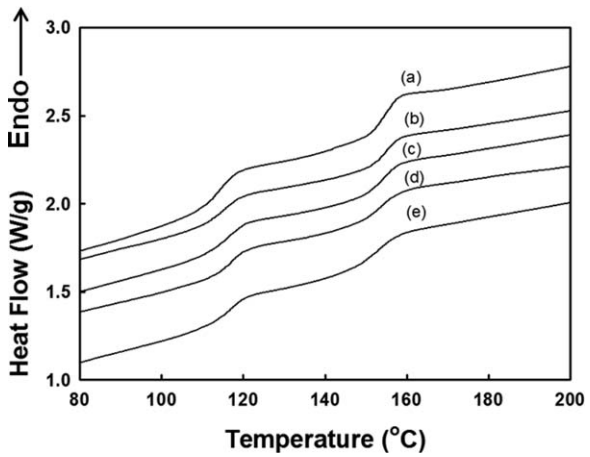

Figure 3. DSC thermograms of PMMA/PMMI (70/30) blends compatibilized with SAN-GMA: (a) 0 phr, (b) 1 phr, (c) 3 phr, (d) 5 phr, (e) 7 phr.

Table I. Glass-Transition Temperatures of PMMA/PMMI (70/30) Blend Compatibilized with the SAN-GMA

SAN-GMA (phr)	T_g (PMMA)	T_g (PMMI)
0	113.8	154.5
1	115.3	154.3
3	115.7	154.0
5	117.7	153.1
7	116.4	153.3

Mechanical Properties

Figure 5(a) shows the flexural strength and Figure 5(b) shows the flexural modulus of PMMA/PMMI blends with SAN-GMA. Figure 5(a) shows that the flexural strength of PMMA/PMMI blends increases from 95.3 to 104.0 MPa as the SAN-GMA content increases up to 5 phr. However, the flexural strength of the blends decreases when a concentration of 7 phr SAN-GMA is used (74.4 MPa). The decrease in flexural strength of the blends after 5 phr could be caused by a plasticizer effect of SAN-GMA. Figure 5(b) illustrates that the flexural modulus of PMMA/PMMI blends increases from 2532.3 to 2711.7 MPa as the SAN-GMA content increases up to 5 phr. However, a decrease in the flexural modulus is observed when 7 phr of SAN-GMA is added (2502.7 MPa), probably also because of a plasticizer effect. Given the results of the morphological, thermal, and mechanical investigations, we conclude that SAN-GMA acts as an effective compatibilizer for PMMA/PMMI (70/30) blends.

Figure 6(a,b) shows the tensile strength and tensile modulus of PMMA/PMMI blends with SAN-GMA. Figure 6(a) shows that the tensile strength of the PMMA/PMMI blends increases from 71.6 to 85.8 MPa as the SAN-GMA content increases up to 5

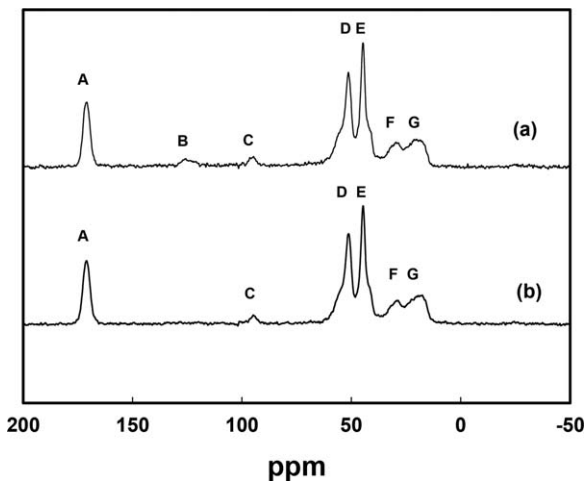

Figure 4. ^{13}C NMR spectra of the PMMA/PMMI (70/30) blends: (a) with SAN-GMA; (b) without SAN-GMA.

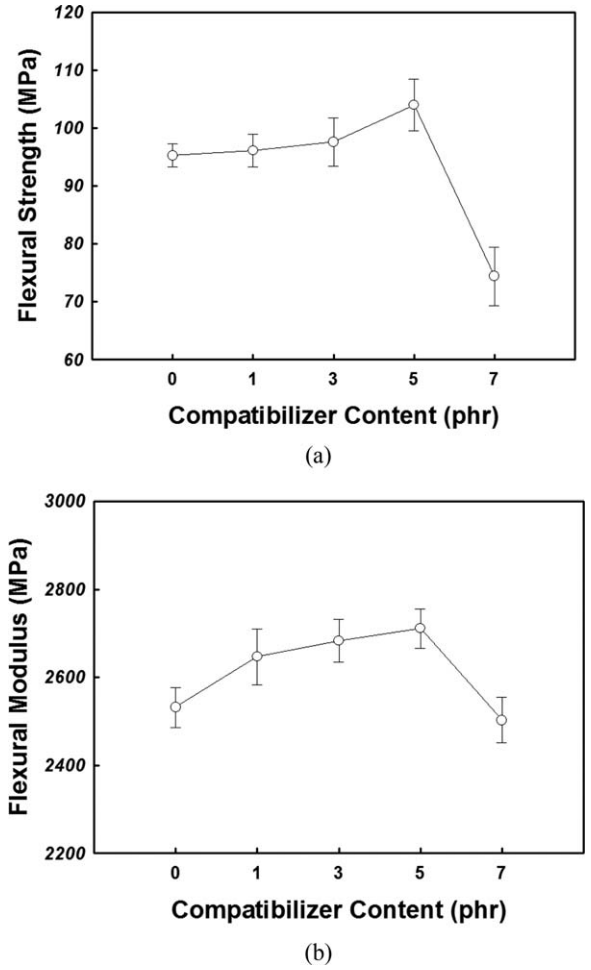

Figure 5. Flexural strength and flexural modulus of PMMA/PMMI (70/30) blends compatibilized with SAN-GMA: (a) flexural strength; (b) flexural modulus.

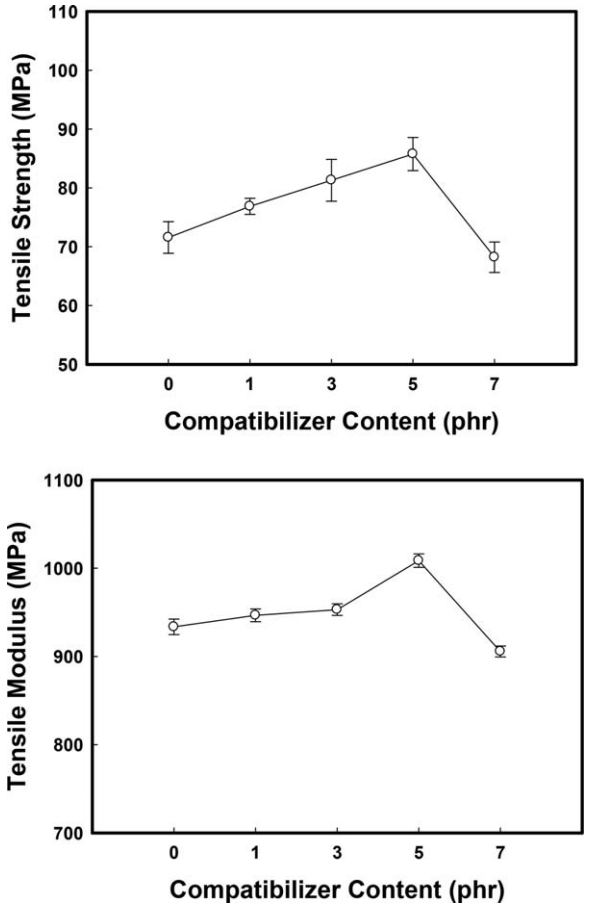

Figure 6. Tensile strength and tensile modulus of PMMA/PMMI (70/30) blends compatibilized with SAN-GMA: (a) tensile strength; (b) tensile modulus.

phr. However, the tensile strength of the blends decreases when a concentration of 7 phr SAN-GMA is used (68.2 MPa). Figure 6(b) illustrates that the tensile modulus of the PMMA/PMMI blends increases from 933.0 to 1008.7 MPa as the SAN-GMA content increases up to 5 phr. However, a decrease in the flexural modulus is observed when 7 phr of SAN-GMA is added (905.6 MPa), probably also because of a plasticizer effect.

Figure 7 shows that the impact strength of the PMMA/PMMI blends increases from 2.83 to 3.99 kg_f cm cm^{-1} as the SAN-GMA content increases up to 5 phr. However, the impact strength of the blends decreases when a concentration of 7 phr SAN-GMA is used (2.85 kg_f cm cm^{-1}). For the PMMA/PMMI (70/30) blend with SAN (5 phr) as a compatibilizer, the flexural strength and tensile strength were measured and found to be 89.2 and 80.1 MPa, respectively, which was lower than the flexural strength (104.0 MPa) and tensile strength (85.8 MPa) of the PMMA/PMMI (70/30) blend with SAN-GMA (5 phr). From Figures 5–7, it is observed that the flexural strength, tensile strength, and impact strength of the PMMA/PMMI (70/30) blends show a maximum when the SAN-GMA is added in the amount of 5 phr. Given the results of the morphological, thermal, and mechanical investigations, it is suggested that SAN-GMA acts as an effective compatibilizer for the PMMA/PMMI (70/30) blends.

The mechanical properties of polymer blends are closely related to the droplet size of the dispersed phase. Figure 8 shows the correlation between mechanical properties and droplet size of

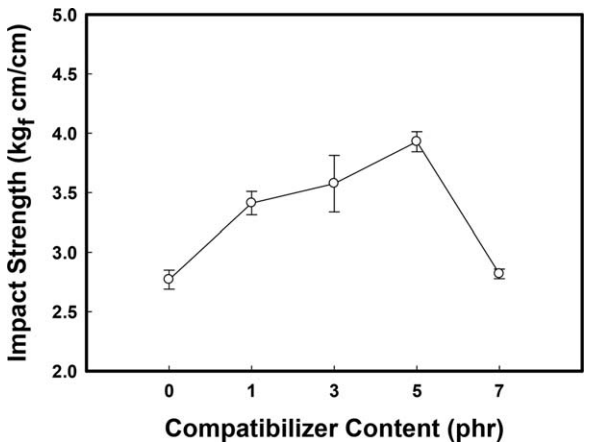

Figure 7. Impact strength of PMMA/PMMI (70/30) blends with SAN-GMA content.

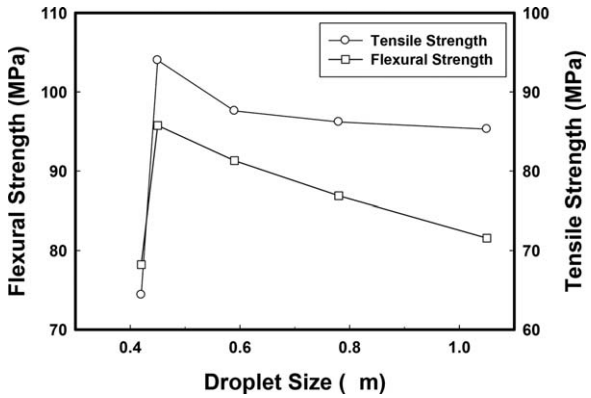

Figure 8. Flexural strength and tensile strength of PMMA/PMMI (70/30) blends with droplet size.

the PMMA/PMMI (70/30) blends with SAN-GMA. As Figure 8 shows, the tensile and flexural strengths decrease with the increase of the PMMI droplet size of the PMMA/PMMI (70/30) blends. The decrease in particle size of the blends suggests an increase in the compatibility between the PMMA and PMMI components. This result is consistent with the results of the mechanical properties of the PMMA/PMMI (70/30) blends shown in Figures 7. For the droplet size of 0.42 μm, the tensile and flexural strengths of the blends decreased, probably because of a plasticizer effect of SAN-GMA when a concentration of 7 phr was added.

Rheology of PMMA/PMMI Blends

Figure 9 shows the storage modulus (G') of neat PMMI, neat PMMA, and PMMA/PMMI (70/30) blends as a function of SAN-GMA content (0, 1, 3, 5, and 7 phr) and frequency. As shown in Figure 9, the storage modulus increases with increasing SAN-GMA content up to 5 phr at all frequencies. The storage modulus decreases at all frequencies when a SAN-GMA concentration of 7 phr is used. At a frequency of 1.0×10^0 rad/s, the storage modulus of the PMMA/PMMI (70/30) blends with SAN-GMA content is shown in Table II.

Figure 10 shows the loss modulus (G'') of neat PMMI, neat PMMA, and PMMA/PMMI (70/30) blends as a function of SAN-GMA content (0, 1, 3, 5, and 7 phr) and frequency. As shown in Figure 10, the loss modulus increases with increasing SAN-GMA content up to 5 phr at all frequencies. The loss modulus decreases when a SAN-GMA concentration of 7 phr is used, which is similar to the storage modulus results shown in Figure 9. At a frequency of 1.0×10^0 rad/s, the loss modulus of PMMA/PMMI (70/30) blends with SAN-GMA content is shown in Table II.

Figure 11 shows the complex viscosity of neat PMMI, neat PMMA, and PMMA/PMMI (70/30) blends as a function of SAN-GMA content (0, 1, 3, 5, and 7 phr) and frequency. In agreement with the storage modulus results, the complex viscosity increases appreciably with the addition of SAN-GMA, except at a SAN-GMA concentration of 7 phr. At a frequency of 1.0×10^0 rad/s, the complex viscosities of PMMA/PMMI (70/30) blends with SAN-GMA concentration are shown in Table II. The increase in complex viscosity from 1.99×10^3 Pa s (0 phr) to 3.40×10^3 Pa s (5 phr) implies an increase in compatibility because of increased interactions between the PMMA and PMMI components. However, a decrease in the complex viscosity is observed at 7 phr SAN-GMA, which is probably due to a plasticizer effect.

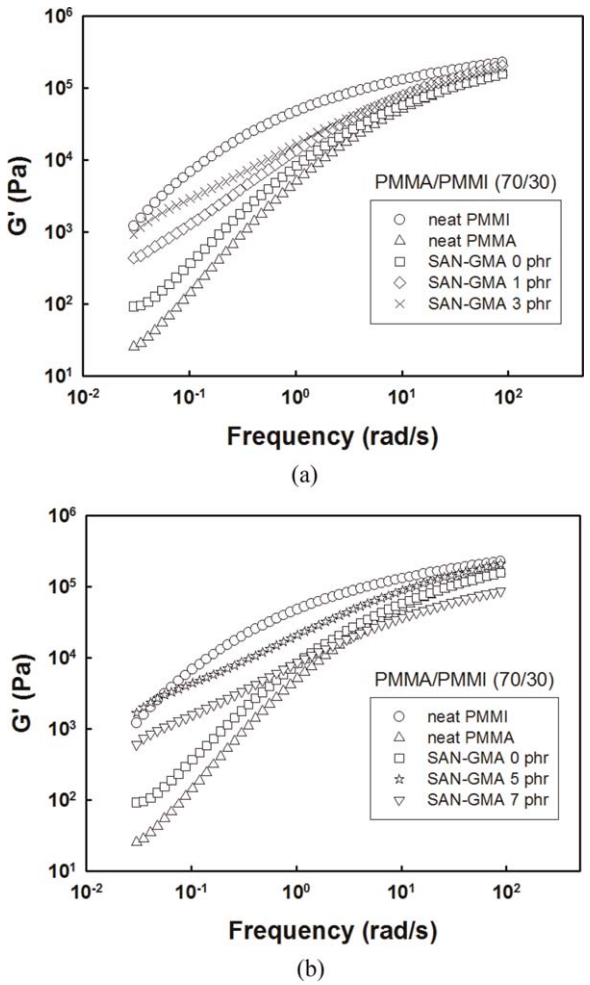

Figure 9. Storage modulus (G') of PMMA, PMMI, and PMMA/PMMI (70/30) blends compatibilized with SAN-GMA : (a) (○) PMMI, (△) PMMA, (□) 0 phr, (◇) 1 phr, (PMMI) 3 phr; (b) (○) PMMI, (△) PMMA, (□) 0 phr, (☆) 5 phr, (▽) 7 phr.

Table II. Storage Modulus, Loss Modulus, and Complex Viscosity at a Frequency of 1.0×10^0 rad/s of the PMMA/PMMI (70/30) Blend Compatibilized with SAN-GMA

SAN-GMA (phr)	Storage modulus (10^4, Pa)	Loss modulus (10^4, Pa)	Complex viscosity (10^3, Pa s)
0	0.84	1.87	1.99
1	1.37	2.58	2.85
3	1.69	2.47	2.92
5	2.10	2.78	3.40
7	0.88	1.19	1.45

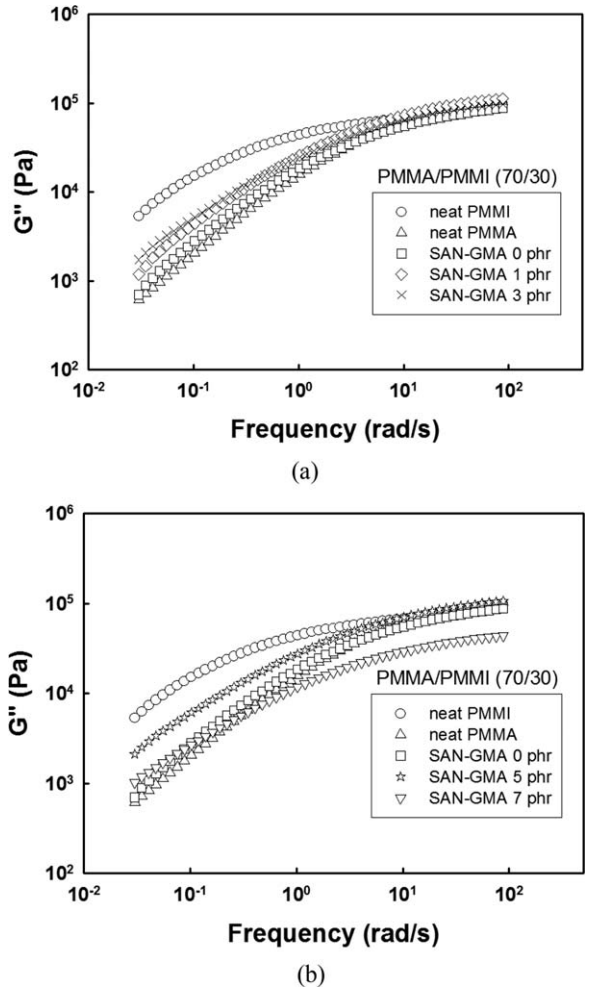

Figure 10. Loss modulus (G'') of PMMA/PMMI (70/30) blends compatibilized with SAN-GMA: (a) (○) PMMI, (△) PMMA, (□) 0 phr, (◇) 1 phr, (×) 3 phr; (b) (○) PMMI, (△) PMMA, (□) 0 phr, (☆) 5 phr, (▽) 7 phr.

Interfacial Tension of PMMA/PMMI Blends

The compatibility of polymers can be assessed by the interfacial tension of the blends. Interfacial tension can be measured by the Palierne emulsion model [eq. (1)][38] and Choi-Schowalter model [eq. (2)][39] using relaxation time.[40–44]

$$\tau_1 = \frac{R_v \eta_m}{4\alpha} \frac{(19K+16)[2K+3-2\varnothing(K-1)]}{[10(K+1)-2\varnothing(5K+2)]} \quad (1)$$

$$\tau_1 = \frac{R_v \eta_m}{4\alpha} \frac{(19K+16)(2K+3)}{40(K+1)} \times \left[1+\varnothing \frac{5(19K+16)}{4(K+1)(2K+3)}\right] \quad (2)$$

where τ_1 is the form relaxation time that is due to the relaxation of the interface between PMMA and PMMI, R_v is the volume-average droplet radius of the droplets in the PMMA/PMMI blend,[44] η_m is the viscosity of the matrix (PMMA), α is the interfacial tension of the PMMA/PMMI blend, Ø is the volume fraction of the dispersed phase (PMMI), and $K = \eta_i/\eta_m$ is the zero-shear viscosity ratio of the droplet and matrix. The relaxation time is obtained from the weighted relaxation spectrum [$\tau H(\tau)$]. The weighted relaxation spectrum [$\tau H(\tau)$] was calculated using the storage modulus (G') and loss modulus (G'') data, which were obtained by ARES measurements.[41–45] Calculation of the weighted relaxation spectrum was carried out using the RSIOrche600 software that was installed in ARES (Piscataway, New Jersey, USA).[35,44]

The weighted relaxation spectra of PMMA and PMMI are shown in Figure 12, which shows that the relaxation times of PMMA and PMMI are found at about 0.4 and 7.1 s, respectively. Since the relaxation times of PMMA and PMMI were so close, the relaxation spectra seen in Figure 12 are partially superimposed. Figure 12 also shows that the peak intensity of the weighted relaxation spectrum of PMMI is quite high compared to that of PMMA, which is understandable since the zero-shear viscosity of PMMI (2.27×10^5 Pa s) is higher than that of PMMA (2.14×10^3 Pa s) (Figure 11).

Figure 13 shows the weighted relaxation spectra of PMMA/PMMI blends with 0, 1, 3, 5, and 7 phr SAN-GMA. In Figure 13, the relaxation spectrum shows only one peak, which is probably because the peaks of PMMA and PMMI and the peak of the long relaxation time associated with the interphase of the PMMA/PMMI blend are so close. From Figure 13 and Table III,

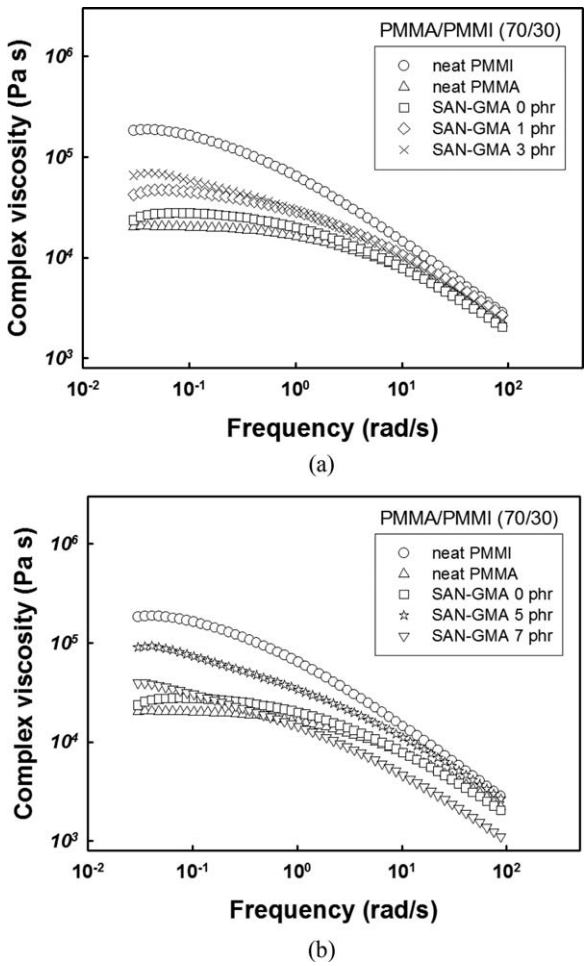

Figure 11. Complex viscosity of PMMA/PMMI (70/30) blends compatibilized with SAN-GMA: (a) (○) PMMI alone, (△) PMMA alone, (□) 0 phr, (◇) 1 phr, (×) 3 phr; (b) (○) PMMI, (△) PMMA, (□) 0 phr, (☆) 5 phr, (▽) 7 phr.

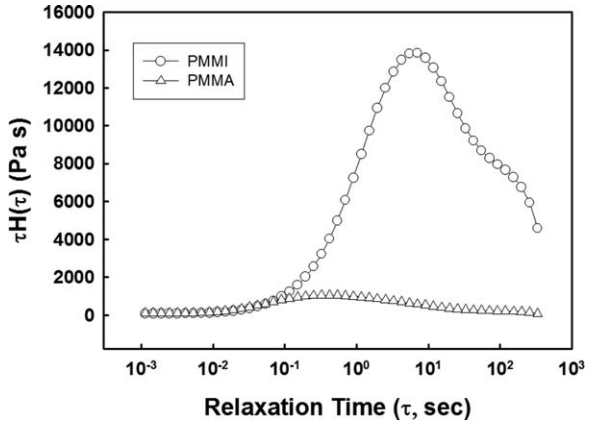

Figure 12. Weighted relaxation spectra of PMMA and PMMI: (○) PMMI; (△) PMMA.

however, it is evident that relaxation time increases with SAN-GMA content (from 3.3 s with 1 phr SAN-GMA to 8.4 s with 7 phr SAN-GMA). When the relaxation time increases, the degree of compatibility of the blend is known to also increase.

Table III also shows the interfacial tension of the PMMA/PMMI blend calculated using the Palierne model. From the Palierne model, the interfacial tension of PMMA/PMMI blends with 1 and 7 phr SAN-GMA are estimated at 31.6 and 6.7 mN/m, respectively, which suggests that compatibility increases with increasing SAN-GMA content. Using the Choi-Schowalter model, the interfacial tensions of the PMMA/PMMI blends with 1 and 7 phr SAN-GMA are estimated at 38.3 and 8.2 mN/m, respectively, which represents a trend similar to the measurements obtained from the Palierne model. When the interfacial tension of the blend decreases, the degree of compatibility of the blend is known to increase. Given the results for the interfacial tension and mechanical properties of the PMMA/PMMI (70/30) blends, we suggest that SAN-GMA is an effective compatibilizer at a concentration of 5 phr; this result is consistent with the results obtained from the morphological and thermal properties of the blends.

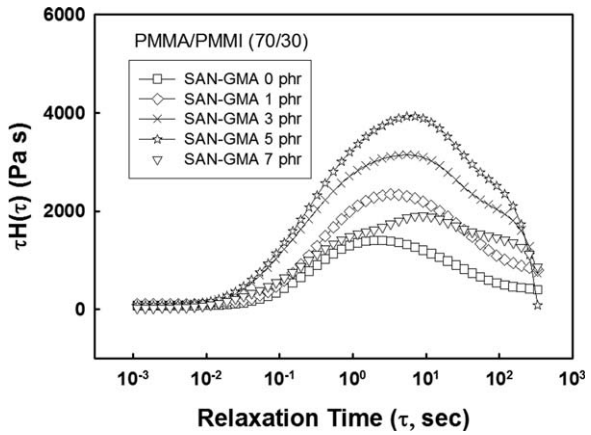

Figure 13. Weighted relaxation spectra of PMMA/PMMI (70/30) blends compatibilized with SAN-GMA: (□) 0 phr, (◇) 1 phr, (×) 3 phr, (◇) 5 phr, (▽) 7 phr.

Table III. Form Relaxation Time (τ_1) and Interfacial Tension (α) for the PMMA/PMMI (70/30) Blend Compatibilized with SAN-GMA

SAN-GMA (phr)	τ_1 (s)	α_1[a] (mN/m)	α_2[b] (mN/m)
0	2.0	72.0	87.3
1	3.3	31.6	38.3
3	5.5	14.4	17.5
5	7.1	8.6	10.4
7	8.4	6.7	8.2

[a] α_1 was calculated from the Palierne emulsion model.
[b] α_2 was calculated from the Choi-Schowalter model.

CONCLUSIONS

In this study, the effects of the compatibilizer SAN-GMA on the morphological, thermal, mechanical, and rheological properties of PMMA/PMMI (70/30) blends were investigated. The morphological studies showed that the droplet size of the dispersed phase (PMMI) decreased with the addition of compatibilizer. In the PPMA/PMMI blend with 5 phr SAN-GMA, the droplet size was 0.42 μm, which is a significant decrease from the droplet size in the blend without compatibilizer (1.05 μm).

Thermal analysis revealed an increase in the T_g of the PMMA-rich phase with the addition of SAN-GMA up to 5 phr. This shift of the T_g of the PMMA-rich phase toward a higher temperature is most likely due to improved compatibility between PMMA and PMMI. The flexural strength and flexural modulus of the PMMA/PMMI blends also increased with the addition of SAN-GMA up to 5 phr. Rheological studies showed that storage modulus, loss modulus, and complex viscosity of the PMMA/PMMI blends increased when SAN-GMA was added up to 5 phr. The increase in complex viscosity of the blends implies an increase in compatibility that is due to an increased interaction between the PMMA and PMMI components.

The interfacial tension of the PMMA/PMMI blend was calculated using the Palierne and Choi-Schowalter models using the weighted relaxation spectrum, which was obtained from the storage modulus and loss modulus of the blend. The results for interfacial tension are consistent with the results obtained from the morphological and mechanical studies. Taken together, the results of the morphological, thermal, mechanical, and rheological studies and the values of the interfacial tension of the PMMA/PMMI (70/30) blends show that the optimum compatibilizer concentration of SAN-GMA is 5 phr.

ACKNOWLEDGMENTS

This work was supported by the Kyung Sung Precision Co. Ltd. in 2015. One author (M. G. Jang) was supported by the global Ph.D. fellowship through the Ministry of Education, South Korea.

REFERENCES

1. Huang, C.; Zhang, L. *J. Appl. Polym. Sci.* **2004**, *92*, 1.
2. Cheng, J.; Zhang, J.; Wang, X. *J. Appl. Polym. Sci.* **2013**, *127*, 3997.

3. Lee, J. G.; Kim, S. H.; Kang, H. C.; Park, S. H. *Macromol. Res.* **2013**, *21*, 349.
4. Feng, C. X.; Huang, T.; Chen, H. M.; Yang, J. H.; Zhang, N.; Wang, Y.; Zhang, C. L.; Zhou, Z. W. *Colloid Polym. Sci.* **2014**, *292*, 3279.
5. Ding, Y.; Chen, G.; Song, J.; Gou, Y.; Shi, J.; Jin, R.; Li, Q. *J. Appl. Polym. Sci.* **2012**, *126*, 194.
6. Madhukar, K.; Sainath, A. V. S.; Bikshamaiah, N.; Srinivas, Y.; Babu, N. M.; Ashok, B.; Kumar, D. S.; Rao, B. S. *J. Therm. Anal. Calorim.* **2014**, *115*, 345.
7. Mallick, S.; Khatua, B. B. *J. Nanosci. Nanotechnol.* **2011**, *11*, 979.
8. El-Salmawi, K.; Abu Zeid, M. M.; El-Naggar, A. M.; Mamdouh, M. *J. Appl. Polym. Sci.* **1999**, *72*, 509.
9. Kumaraswamy, G. N.; Ranganathaiah, C.; Deepa Urs, M. V.; Ravikumar, H. B. *Eur. Polym. J.* **2006**, *42*, 2655.
10. Cocco, D. R.; de Carvalho, F. P.; Felisberti, M. I. *J. Appl. Polym. Sci.* **2013**, *130*, 654.
11. Kim, W. N.; Burns, C. M. *Macromolecules* **1987**, *20*, 1876.
12. Ray, S. S.; Bousmina, M. *Macromol. Rapid Commun.* **2005**, *26*, 450.
13. Lee, W. F.; Lai, C. C. *J. Appl. Polym. Sci.* **1997**, *66*, 761.
14. Pal, A.; Khare, P. K. *Bull. Mater. Sci.* **2013**, *36*, 115.
15. Kerboua, N.; Cinausero, N.; Sadoun, T.; Lopez-Cuesta, J. M. *J. Appl. Polym. Sci.* **2010**, *117*, 129.
16. Al-Mulla, A.; Shaban, H. I. *Polym. Bull.* **2007**, *58*, 893.
17. Auliawan, A.; Woo, E. M. *J. Appl. Polym. Sci.* **2012**, *125*, E444.
18. Ayutthaya, W. D. N.; Poompradub, S. *Macromol. Res.* **2014**, *22*, 686.
19. Anakabe, J.; Huici, A. M. Z.; Eceiza, A.; Arbelaiz, A. *J. Appl. Polym. Sci.* **2015**, *132*, 42677.
20. Wu, J. H.; Kuo, M. C.; Chen, C. W. A. *J. Appl. Polym. Sci.* **2015**, *132*, 42378.
21. Zhang, C.; Yi, X. S.; Yui, H.; Asai, S.; Sumita, M. A. *J. Appl. Polym. Sci.* **1998**, *69*, 1813.
22. Zsoldos, G. E.; Kollar, M. *J. Thermal. Anal. Calorim.* **2015**, *119*, 63.
23. D'orazio, L.; Guarino, R.; Mancarella, C.; Martuscelli, E.; Cecchin, G. *J. Appl. Polym. Sci.* **1997**, *66*, 2377.
24. Chatterjee, A.; Mishra, S. *Macromol. Res.* **2013**, *21*, 474.
25. Yao, M.; Deng, H.; Mai, F.; Wang, K.; Zhang, Q.; Chen, F.; Fu, Q. *eXPRESS Polym. Lett.* **2011**, *5*, 937.
26. Yoo, S. J.; Lee, S. H.; Jeon, M.; Lee, H. S.; Kim, W. N. *Macromol. Res.* **2013**, *21*, 1182.
27. Liau, W. B.; Chang, C. F. *J. Appl. Polym. Sci.* **2000**, *76*, 1627.
28. Luo, C.; Chen, W.; Gao, Y. *J. Appl. Polym. Sci.* **2015**, *132*, DOI: 10.1002/app.41705.
29. Yang, D.; Xu, H.; Wu, Y.; Wang, J.; Xu, Z.; Shi, W. *J. Polym. Res.* **2013**, *20*, 236.
30. Ghavidel, A. K.; Azdast, T.; Shabgard, M.; Navidfar, A.; Sadighikia, S. *J. Appl. Polym. Sci.* **2015**, *132*, DOI: 10.1002/app.42671.
31. Yang, J.; Yan, X.; Wu, M.; Chen, F.; Fei, Z.; Zhong, M. J. *Nanopart. Res.* **2012**, *14*, 717.
32. Wochnowski, C.; Hanada, Y.; Cheng, Y.; Metev, S.; Vollertsen, F.; Sugioka, K.; Midorikawa, K. *J. Appl. Polym. Sci.* **2006**, *100*, 1229.
33. Eklind, H.; Schantz, S.; Maurer, F. H. J.; Jannasch, P.; Wesslen, B. *Macromolecules* **1996**, *29*, 984.
34. Barral, L.; Cano, J.; Lopez, J.; Lopez-Bueno, I.; Nogueira, P.; Torres, A.; Ramirez, C.; Abad, M. J. *Thermochim. Acta* **2000**, *344*, 127.
35. Fowler, M. E.; Barlow, J. W.; Paul, D. R. *Polymer* **1987**, *28*, 1177.
36. Li, Y.; Shimizu, H. *ACS Appl. Mater. Interfaces* **2009**, *1*, 1650.
37. Koenig, J. L. Spectroscopy of Polymers; Americal Chemical Society: Washington, DC, **1992**.
38. Palierne, J. F. *Rheol. Acta* **1990**, *29*, 204.
39. Choi, S. J.; Schowalter, W. R. *Phys. Fluids* **1975**, *18*, 420.
40. Olley, P.; Coates, P. D. J. *Non-Newtonian Fluid Mech.* **1997**, *69*, 239.
41. Honerkamp, J.; Weese, J. *Rheol. Acta* **1993**, *32*, 65.
42. Sung, Y. T.; Han, M. S.; Hyun, J. C.; Kim, W. N.; Lee, H. S. *Polymer* **2003**, *44*, 1681.
43. Yoo, T. W.; Yoon, H. G.; Choi, S. J.; Kim, M. S.; Kim, Y. H.; Kim, W. N. *Macromol. Res.* **2010**, *18*, 583.
44. Lee, J. B.; Lee, Y. K.; Choi, G. D.; Na, S. W.; Park, T. S.; Kim, W. N. *Polym. Degrad. Stabil.* **2011**, *96*, 553.
45. Tschoegl, N. W. The Phenomenological Properties of Polymers; Wiley: New York, **1980**.